Anal. Chem. **2002,** *74,* 5257−5262

Separate Detection of BTX Mixture Gas by a Microfluidic Device Using a Function of Nanosized Pores of Mesoporous Silica Adsorbent

Yuko Ueno,* Tsutomu Horiuchi, Masato Tomita,† and Osamu Niwa

NTT Lifestyle and Environmental Technology Laboratories, Atsugi, Kanagawa 243-0198, Japan

Hao-shen Zhou,*, Takeo Yamada, and Itaru Honma

National Institute of Advanced Industrial Science and Technology, Tsukuba, Ibaragi 305-8568, Japan

We achieved separate detection of the components of 10 ppm of a benzene, toluene, and *o*-xylene mixture gas by using mesoporous silica powder incorporated in our microfluidic device. The device consists of concentration and detection cells formed of 3 cm × 1 cm Pyrex plates. We first introduced the mixture gas into the concentration cell where it was adsorbed on an adsorbent in a channel formed in the cell. We then raised the temperature using a thin-film heater and introduced the desorbed gas into the detection cell. Here, we measured the changes in the absorption spectra of the mixture gas in the detection cell. We found that the mixture ratio of the compounds in the desorbed gas varies with time because the thermal desorption property of each compound is different from that of the adsorbent. We analyzed the thermal desorption mechanism by comparing two types of silica adsorbents with different pore structures. We found that an adsorbent that has pores with a periodic and uniform nanosized column shape provides better component separation. We concluded that the uniform pore structure might cause the adsorbate molecules to exhibit a homogeneous adsorption state thus revealing the desorption properties of the gas more clearly.

Airborne benzene, toluene, and xylenes (BTX) are volatile organic compounds (VOCs) that are of significance as regards environmental health due to their toxicity and mutagenetic or carcinogenetic properties even at parts-per-billion concentrations. In particular, benzene is classified as a human carcinogen for all exposure routes and is a risk factor for leukemia and lymphomas.[1] Habitual inhalation of toluene or xylenes may induce brain function disturbances in addition to kidney and liver damage.[2] The body of knowledge on the carcinogenic effects of toluene and xylenes is still based on inadequate evidence.[3] The toxicities of BTX vary greatly and regulations relating to them also differ. The regulated average annual concentrations of benzene in the air are 1, 3, and 5 $\mu g/m^3$ (0.33, 1.0, and 1.6 ppb) in the United States,[4] Japan,[5] and the European Union,[6] respectively. The guidelines for the upper indoor concentration limits of toluene and xylenes in Japan are 260 and 870 $\mu g/m^3$ (0.07 and 0.20 ppm), respectively. In contrast, BTX are the main components of automobile exhaust gases from gasoline engines. The main source of benzene emissions (more than 80%) is automobile exhaust and traffic-related processes.[7] Benzene is emitted into the air not only due to the original benzene content of the gasoline but because it is also formed during the combustion process itself. Toluene and xylenes are also major constituents of gasoline and thus automobile exhaust. However, unlike benzene, they are also used in large quantities as solvents. Because their concentration in the air depends on time and location, it is important to determine the concentration of every compound in the air separately for on-site field monitoring.

A portable system is required for on-site monitoring that can detect each BTX species. However, the widely used conventional miniature devices for VOC detection, for example, photoionization detectors or surface acoustic wave detectors, have very limited ability to recognize each compound individually. Therefore, quantitative measurement of each gas is difficult. Recently, we developed a microfluidic device designed to detect and identify BTX in the air.[8,9] Our device is composed of concentration and detection cells with peripheral devices. Each cell is 3 cm × 1 cm.

* Corresponding authors: (E-mail) ueno@aecl.ntt.co.jp; (Fax) +81-46-270-2320. (E-mail) hs.zhou@aist.go.jp; (Fax) 81-298-61-5829.

† Current address: Corning Japan K. K., Ogasa-gun, Shizuoka 437-1397, Japan.

(1) See, for example: *Carcinogenic Effects of Benzene: An Update*, 1998; EPA/60/P-97/001F.; U. S. Environmental Protection Agency, U.S. Government Printing Office: Washington, DC, 1998.

(2) See, for example: *Environmental Health Criteria 52; Toluene*, 1985; WHO: Geneva, 1985, *Environmental Health Criteria 190; Xylenes*, 1997; WHO: Geneva, 1997.

(3) Snyder, R.; Kalf, G. *Crit. Rev. Toxicol.* **1994**, *24* (3), 177.

(4) *National Air Toxics Program: The Integrated Urban Strategy, Report to Congress*, 2000; EPA-453/R-99-007; U.S. Environmental Protection Agency, U.S. Government Printing Office: Washington, DC, 2000.

(5) *Environmental Quality Standards in Japan, Air Quality, Environmental Quality Standards of Benzene, Trichloroethylene and Tetrachloroethylene*, 1997; http://www.env.go.jp/en/lar/regulation/aq.html; Ministry of the Environment, Government of Japan.

(6) *Are we moving in the right direction? TERM 2000*. Environmental Issues Series 12, 2000; http://reports.eea.eu.int/ENVISSUENo12/en/page008.html; European Environment Agency, 2000.

(7) *9th Report on Carcinogens*: http://ehis.niehs.nih.gov/roc/toc9.html; U.S. Department of Health and Human Services Public Health Service, 2001.

(8) Ueno, Y.; Horiuchi, T.; Morimoto, T.; Niwa, O. *Anal. Chem.* **2001**, *73*, 4688.

(9) Ueno, Y.; Horiuchi, T.; Niwa, O. *Anal. Chem.* **2002**, *74*, 1712.

10.1021/ac0201732 CCC: $22.00
Published on Web 09/20/2002

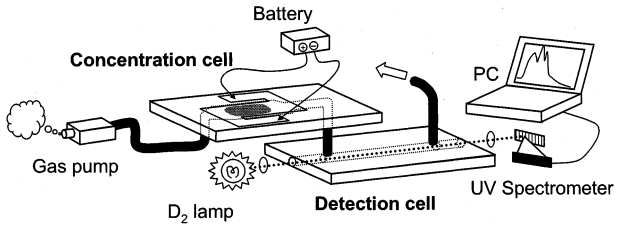

Figure 1. Schematic view of microfluidic device with peripheral devices.

To measure BTX gases, we first introduce polluted air into the concentration cell by using a palm-size pump, and the gas is adsorbed on an adsorbent in a channel formed in the cell. After sampling the gas for a specified time, we raise the temperature using a thin-film heater in order to desorb the concentrated gas from the adsorbent. We then introduce the desorbed gas into the detection cell, which is aligned between a light source and a spectrometer, and measure the absorption spectra of the gas. We realized a 0.05 ppm detection limit for toluene gas as an example BTX with a sampling time of 30 min. We also confirmed that our microfluidic device is capable of detecting benzene and *o*-xylene in the same way. We can identify each compound by observing their specific peaks in the spectra. Moreover, it is necessary to improve BTX separation by using the microfluidic device to detect each component in the BTX mixture gas quantitatively, as required for field monitoring.

In this paper, we report the separate detection of the components of 10 ppm of a benzene, toluene, and *o*-xylene mixture gas by using mesoporous silica incorporated in our microfluidic device. We found that the shapes of the detected spectra of the mixture gas differ significantly with time due to changes in the mixture ratio, which depends on the thermal desorption property of the gases from the adsorbent. We also found that we can obtain a better separation of BTX by using highly ordered mesoporous silica as an adsorbent due to a function of its nanosized pores. We have succeeded in detecting the individual components in BTX mixture gas at ppm levels with this device.

EXPERIMENTAL SECTION

Setup. Figure 1 shows a schematic view of the microfluidic device with peripheral devices. To provide an artificial environment of BTX-polluted air, we prepared benzene, toluene, and *o*-xylene mixture gases by diluting commercial-grade toluene (50 ppm), benzene (50 ppm), and *o*-xylene (50 ppm) gases with nitrogen in a gas blender consisting of mass-flow meters (Estec, SEC-400). We introduced this BTX mixture gas into the concentration cell with a Bimor pump (Kyokko Co., Ltd., BPF-465P) 72 mm × 72 mm × 32 mm in size. Each part of the pump that came into contact with the flowing gas was made of fluoroplastic. We were able to vary the gas flow rate by changing the output frequency of the pump. Here, we set the output frequency at 100 Hz, which gave us a flow rate of $\sim 1.1 \times 10^{-1}$ cm^3/s at the point furthest downstream from the device. The BTX mixture gas was first introduced into the concentration cell and then adsorbed by the adsorbent in a channel formed in the cell. The adsorbents we used were (a) commercially obtained amorphous silicon dioxide powder (Kanto Chemical Co. Inc.) and (b) nonionic triblock copolymer templated self-ordered mesoporous silicate powder SBA-15, which was synthesized by a method described elsewhere.[10] We denote the above adsorbents as SDP and SBA-15, respectively.

We packed ~5 mm of the channel with ~1.5 mg of SDP and ~0.5 mg of SBA-15. We sampled the BTX mixture gas for a certain time and then we raised the temperature using a thin-film heater so that the concentrated BTX mixture gas was desorbed from the adsorbent in accordance with the particular desorption temperatures of benzene, toluene, and *o*-xylene. We set the applied voltage at 14.5 V, which we adjusted to increase the temperature at the adsorbent to ~200 °C. We measured the temperature at the adsorbent by using an infrared thermometer (Keyence, IT2-02 controlled by IT2-50). The measurement spot size was $\phi = 1.2$ mm. We then introduced desorbed gas into the detection cell along with a carrier gas, namely, the original BTX mixture gas we used as a sample. In the detection cell, we measured the absorption spectra of the desorbed gas by using optical fibers fixed at the edges of a channel aligned between a light source and a spectrometer, respectively. Because the BTX absorption spectra spread over the UV region, we used a 30-W deuterium (D_2) lamp (Soma Optics) as the light source. We measured the absorption spectra using a UV spectrometer (Fastevert S-2400, Soma Optics) that was specially modified for this device. We have described the details of the structures of the concentration and detection cells and the fabrication process elsewhere.[9]

Measurement. We measured the changes in the absorption spectra against time obtained in the detection cell when using SDP and SBA-15 as adsorbents for the detection of BTX mixture gas. The concentrations of the benzene, toluene, and *o*-xylene in the BTX mixture gas were each 10 ppm. We sampled the BTX mixture gas for 30 min for each adsorbent at the flow rate described above (1.1×10^{-1} cm^3/s). We measured the background spectrum prior to each measurement. We set the time at which we turned the heater on at zero seconds ($t = 0$). We set the time for which the detector was exposed to UV light at 500 ms, which is the maximum value before the detector sensitivity saturates. We accumulated 10 sets of 500-ms exposure data. Thus, the total time required to measure each spectrum was 5 s. We therefore define absorbance at t as the average value obtained in 5 s, from ($t - 2.5$) to ($t + 2.5$). We measured the absorption spectra at 5-s intervals. To study the changes in shorter time steps, we repeated the measurement, on this occasion delaying the measurement starting time by 2.5 s, and overlaid the two results. Thus, we obtained the absorption spectra every 2.5 s.

Before measuring the BTX mixture gas, we measured standard spectra of benzene, toluene, and *o*-xylene. To obtain them, we measured the changes in the absorption spectra against time for single compounds of benzene, toluene, and *o*-xylene. The concentration of each original gas was 30 ppm, and we sampled the gas for 30 min. The spectra with the strongest absorbance in the time series were observed at $t = 10.0$, 12.5, and 15.0 s, for benzene, toluene, and *o*-xylene, respectively. We thus employed these three spectra as standard spectra for benzene, toluene, and *o*-xylene.

Separation of a Mixture Gas Spectrum into Single-Component Spectra. We denote the standard spectra of benzene, toluene, and *o*-xylene as *B*, *T*, and *X*, respectively. Each standard spectrum consisted of 700 data that corresponded to the absor-

(10) Zhao, D.; Huo, Q.; Feng, J.; Chmelka, B. F.; Stucky, G. D. *J. Am. Chem. Soc.* **1998**, *120*, 6024.

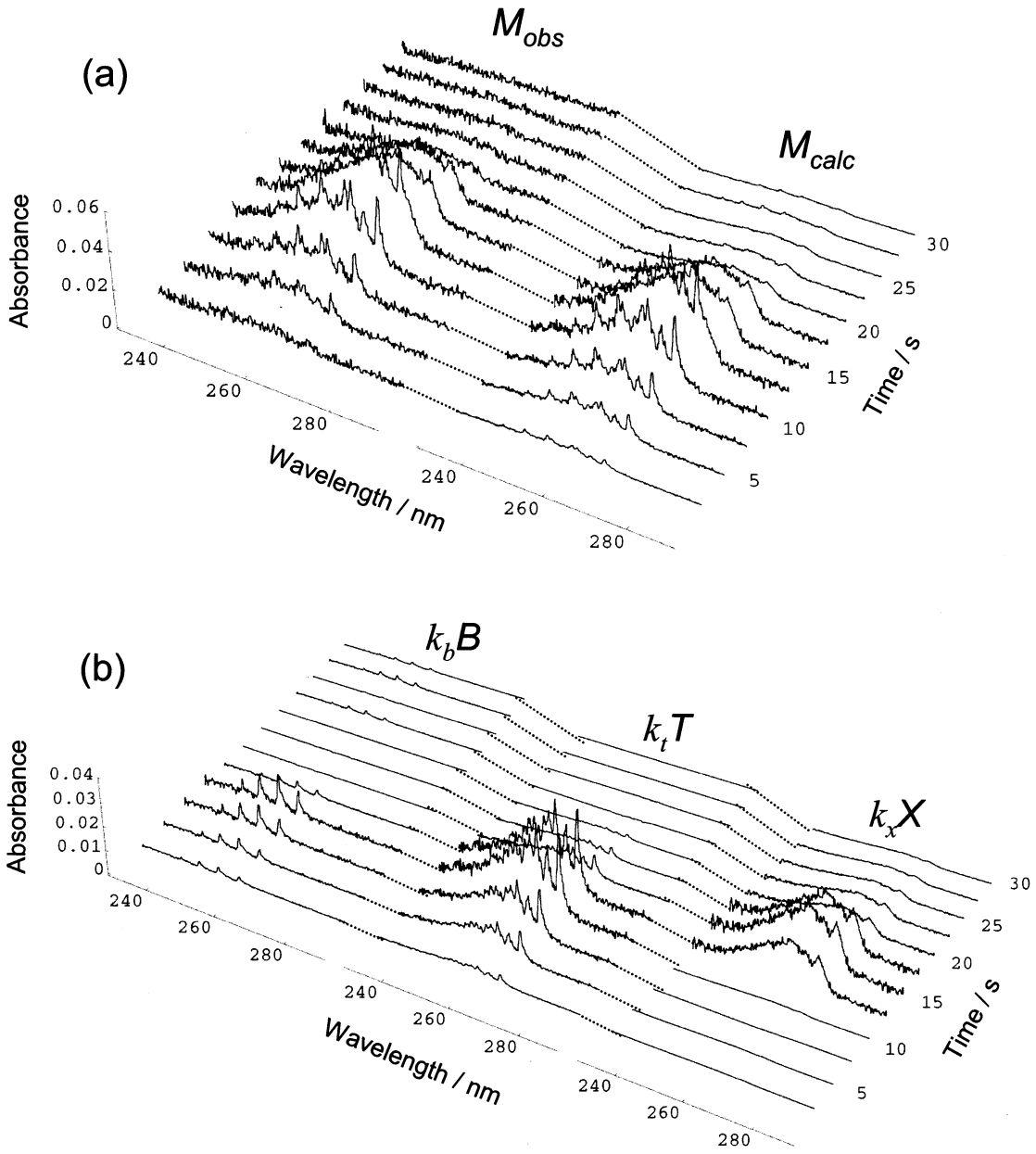

Figure 2. Changes in M_{obs} against time and the corresponding M_{calc} obtained by calculating eq 4 when SDP is used as the adsorbent (a) and each component (k_xB, k_tT, and k_xX) that composes M_{calc} (b).

bance in the 230.1−300.0-nm region in 0.1-nm steps. We can calculate the theoretical spectrum for any mixing ratio of BTX mixture gas (M_{calc}) by using B, T, and X multiplied by coefficients that correspond to the ratio of the benzene, toluene, and *o*-xylene (k_b, k_t, k_x) in the mixture gas by using the following eq 1.

$$M_{calc} = kM_{st} \tag{1}$$

Here, k and M_{st} are 1×3, 3×700 rectangular matrixes defined respectively as follows.

$$k = (k_b, k_t, k_x) \tag{2}$$

$$M_{st} = \begin{bmatrix} B \\ T \\ X \end{bmatrix} \tag{3}$$

The spectrum of the measured BTX mixture gas (M_{obs}) also consisted of 700 data that corresponded to the absorbance in the 230.1−300.0-nm region in 0.1-nm steps (1×700 matrix).

By choosing k using the following equation, we minimize the error between the calculated and observed spectra ($|M_{calc} - M_{obs}|$)

$$k = M_{obs} \cdot M_{st}^{-1} \tag{4}$$

Here M_{st}^{-1} is the pseudoinverse matrix of M_{st}. Thus, by calculating eq 4, we obtain k_b, k_t, and k_x that correspond to the most likely ratio of the benzene, toluene, *o*-xylene in the mixture gas, and they best reproduce M_{obs}.

RESULTS AND DISCUSSION

Figure 2a shows the results of a BTX mixture gas measurement with SDP as the adsorbent. The measurement reveals the

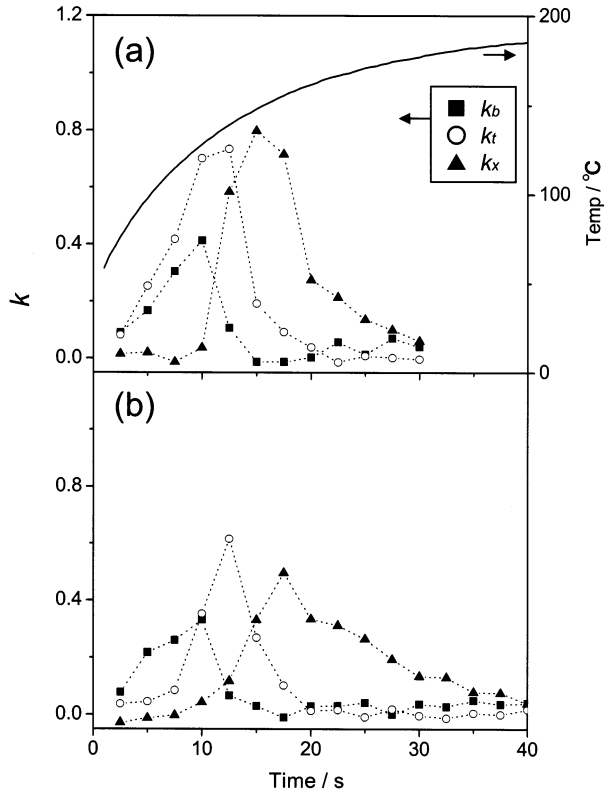

Figure 3. Changes in k_b, k_t, and k_x against time when SDP (a) and SBA-15 (b) are used. The thermal characteristic of the concentration cell with SDP is superimposed on the plot (boldface line).

changes in M_{obs} against time and the corresponding M_{calc} obtained by calculating eq 4. The M_{obs} shapes changed greatly with time. Every M_{obs} was well reproduced by M_{calc}. However, when the M_{obs} absorbance was close to the background level (t = 2.5 s and t = 22.5−30.0 s), the signal-to-noise ratio (S/N) of M_{obs} and M_{calc} differed greatly because the S/N of M_{calc} is determined by that of the standard spectra while S/N of M_{obs} depends on its own absorbance. The S/N at the M_{obs} peak is ∼30 in this case. Therefore, the estimated limit of the separable concentration of BTX gas, where the S/N = 3, is ∼1 ppm here. When we measure actual environmental gases, the limit may worsen. To avoid any reduction in adsorbent capacity as a result of the adsorption of other gases, for example, water, aliphatic compounds, and polycyclic aromatic hydrocarbons, during sampling, we can employ a multibed adsorption method that combines various adsorbents in the same sampling channel. This approach is normally used to adjust the adsorption and desorption capacity in relation to the analytes of interest. Since we measured only the 230−275-nm region, other gases did not interfere with the separation of a mixture gas spectrum into single BTX component spectra. In addition, we were able to avoid the accumulation of water on the adsorbent by carrying out the thermal desorption at ∼200 °C.

Figure 2b shows the spectra separated into each component (k_xB, k_tT, and k_xX) of M_{calc}. The device response intensity of benzene, toluene, and *o*-xylene differed with time independently of each other, although the qualitative behavior of each compound was the same: namely, it first increased, then reached its maximum, and then decreased to the background level. However, the time at which they reached maximum and the time scales of the observed responses both differed with the compounds. We assume that the difference in the device response with the different compounds was due to the difference between the thermal desorption characteristics of each compound and the adsorbent. We thought that the thermal desorption characteristics must differ with the adsorbent. We therefore compared the device responses of SDP and SBA-15.

Table 1. Time at Which the Benzene, Toluene, and *o*-Xylene Signals Reach Their Median Value

	time at median (s)		
	benzene	toluene	*o*-xylene
SDP	9.0	10.6	16.3
SBA-15	9.2	12.2	21.1

Table 2. Parameters of the Porosity of SDP and SBA-15.

	S_{BET} (m^2/g)[a]	V_{pore} (dm^3/g)[b]	D_{pore} (nm)
SDP	268	65	1.36[c]
SBA-15	723	528	6.74[d]

[a]BET surface area. [b]Total pore volume. [c]Pore diameter size from *t*-plot method. [d]Pore diameter size from the DH plot method.

Figure 3 compares changes in k_b, k_t, and k_x with time when using SDP (a) and SBA-15 (b). The thermal characteristic of the concentration cell with SDP was superimposed on the plot (boldface line). We have not shown the thermal characteristic of the concentration cell with SBA-15 because it was almost the same as the result obtained with SDP.

Because the adsorption mechanism of aromatic molecules on silica is via hydrogen bonding between the π-system and silanol on the silica surface,[11] the interaction between the adsorbate molecules and the silica surface may be similar for benzene, toluene, and *o*-xylene. Therefore, the differences between the desorption properties should also small. However, there was a clear difference between the three compounds. This also indicates that its fast response gives a microfluidic system an advantage with regard to observing such small differences in the thermal desorption property.

The order of the compounds detected initially was the same for both SDP and SBA-15, namely, benzene, toluene, and then *o*-xylene. Because the interaction between the adsorbate molecules and the silica surface is almost the same, for molecules adsorbed on a monolayer, the compound that has the larger vapor pressure may desorb more easily from the surface with an increase in temperature. The saturated vapor pressure of benzene, toluene, and *o*-xylene at 25 °C are 1.27 × 10^5, 3.79 × 10^4, and 1.28 × 10^4 Pa, respectively. By contrast, the molecules adsorbed by the multilayer interact with each other as well as in a liquid phase. Therefore, the compound with the lower boiling point completes its vaporization at the lower temperature. The boiling points of benzene, toluene, *o*-xylene are 80.1, 110.6, and 144.4 °C, respectively. Previous studies confirmed that the adsorption/desorption properties of VOCs in relation to microporous materials are

(11) For example: Burneau, A.; Gallas, J.-P. In *The Surface Properties Of Silicas*; Legrand, A. P., Ed.; John Wiley & Sons Ltd.: New York, 1998; p 147. Davydov, V. Ya. In *Adsorption On Silica Surfaces*; Papirer, E., Ed.; Marcel Dekker: New York, 2000; p 35.

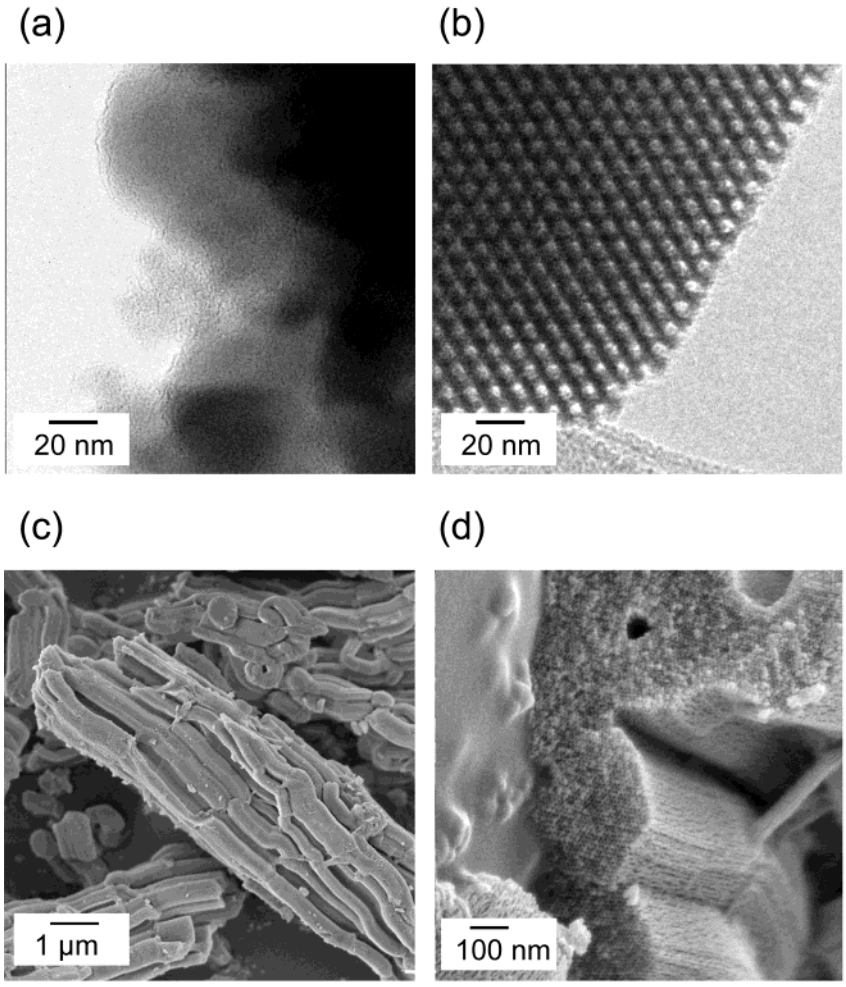

Figure 4. TEM images of SDP (a) and SBA-15 (b) and SEM images of SBA-15 (c, d). The section view (b, c) and the side view (d) of the pores of SBA-15 are displayed.

correlated with the boiling point, vapor pressure, and heat of vaporization.[12] We therefore analyzed the effect of temperature on the desorption properties by comparing the changes in k_b, k_t, and k_x with the thermal characteristics of the concentration cell. The temperatures at the adsorbent increased steeply and reached ~200 °C in ~40 s due to the small heat capacity of the thin-film heater. With SDP, k_b and k_t were detected from $t = 2.5$ s (~60 °C) and then k_x increased from $t = 10.0$ s (~130 °C). With SBA-15, k_b was detected from $t = 2.5$ s (~60 °C), and then k_t and k_x were detected from $t = 7.5$ (~110 °C) and $t = 10.0$ s (~130 °C), respectively. This indicates that the vapor pressure and boiling point are important factors that affect the thermal desorption property.

We then analyzed the difference between the desorption properties of the adsorbents in detail. Table 1 shows the time at which the benzene, toluene, and *o*-xylene signals reach their median. The separation of benzene−toluene and that of toluene−*o*-xylene was improved by 1.6 to 3.0 (188%) and 5.7 to 8.9 s (156%), respectively. Moreover, the shapes of the desorption profiles were also different. SBA-15 provided sharper shapes around the toluene and *o*-xylene peaks while SDP provided broader shapes. This indicates that SBA-15 provides response curves with much greater component separation than SDP. However, the benzene, toluene, and *o*-xylene signals took longer to reach their mean values with SBA-15 than with SDP. This shows that the interaction between the adsorbate gases and the surface is stronger with SBA-15 than with SDP. This may result in an undesirable long tail for *o*-xylene with SBA-15. This must be improved by optimizing either the flow rate or the temperature range of the heat cycle used in the measurements. To analyze the mechanisms that cause the difference in the desorption profiles, we first measured the infrared and Raman spectra of SDP and SBA-15 to determine whether their surface chemical groups are different. However, we were unable to find significant differences in their chemical compositions. We therefore assumed that the differences in the separation of the components and the shapes of the desorption profiles could be ascribed to the structural difference between the pores of the two adsorbents.

Table 2 summarizes the porosity parameters of SDP and SBA-15. We measured the nitrogen adsorption desorption isotherms at 77 K (liquid nitrogen temperature) and calculated the Brumauer−Emmett−Teller (BET) surface area (S_{BET}), the total pore volume (V_{pore}), and the pore diameter (D_{pore}) using either the Dollimore−Heal (DH) plot method[13] or the *t*-plot method.[14] The

(12) Senf, L.; Frank, H. *J. Chromatogr.* **1990**, *520*, 131. Serbezov, A.; Sotirchos, S. V. *Sep. Purif. Technol.* **2001**, *24*, 343.

(13) Dollimore, D.; Heal, G. R. *J. Appl. Chem.* **1964**, *14*, 109.
(14) Lippens, B. C.; de Boer, J. H. *Catalysis* **1965**, *4*, 319.

results were consistent with the previous studies.[10,15] SBA-15 has much larger S_{BET} and V_{pore} values than SDP. Although SDP has a small capacity, it was sufficiently large to adsorb the amount of the sample that we concentrated on the adsorbents, because the total amount of BTX gases was less than 25 μg here while the capacity of SDP calculated from V_{pore} was ∼360 μg. Moreover, the D_{pore} of SBA-15 was ∼10 times larger than that of SDP and this may be the most important factor as regards the thermal desorption property. To compare the structural difference in detail, we measured transmission electron micrograph (TEM) and scanning electron microscope (SEM) images of SDP and SBA-15. Panels a and b of Figure 4 show TEM images of SDPand SBA-15, respectively. Panels c and d of Figure 4 show SEM images of SBA-15. The pore structure of SDP was not clearly observed because none of the pores were sufficiently large (>1 nm). The TEM image b clearly shows a section view of the honeycomblike hexagonal structure of the pores of SBA-15. The pores were ∼7 nm in diameter, thus corresponding with the results we obtained from isothermal measurements. The pores arrayed with the same orientation. This uniform structure was also observed in the SEM image c. The SEM image d shows a side view of the honeycomb-like hexagonal structure of the pore. Because the length of the long axis of the pores was about 1−3 μm, the pore was cylindrical and took the form of a nanosized capillary column.

We then considered the thermal desorption mechanism of SBA-15 as follows: molecules that desorb from the inner surface of the nanosized capillary column would have many opportunities to collide with the wall of the column before they reach the outside of the pore. Once a molecule has collided with the column, it must interact with the surface of the column and desorb from the wall again. The SBA-15 pores have the Knudsen number K, that is expressed by I/d, and that is much larger than 1. Here, I is the mean free path of the molecules and d is the pore radius. Thus, we can treat the desorbed molecules as a free molecular flow and the collision between molecules is negligible in this nanosized capillary column. Therefore, even if the interaction between the adsorbate molecules and the silica surface may be similar for benzene, toluene, and *o*-xylene, as described above, the small difference may be enhanced by the repetition of this adsorption/desorption process. Because the pores of SDP do not have such a columnar structure, the effect of the enhancement must be small. Thus, SBA-15 provides better separation for each component than SDP.

Last, we also measured the effects of concentration on signal intensity. Compared with mixture gases containing 10 ppm of each constituent, the signal intensities of the benzene, toluene, and *o*-xylene in the mixture gases (benzene:toluene:*o*-xylene = 10:5:2.5/ppm; benzene:toluene:*o*-xylene = 2.5:5:10/ppm) changed to 100, 72, and 37% and 37, 76, and 87%, respectively. It is notable that the signal intensities of 5 ppm of toluene were similar even though we changed the benzene and *o*-xylene concentrations. In addition, the nonlinear behavior of the signal intensity in relation to the concentration corresponds well with the toluene calibration curve we measured in our previous study:[9] the signal intensity of 5 ppm toluene was ∼76% that of 10 ppm toluene. The shapes of the desorption profiles of each compound were similar with different concentration and mixture ratios. This indicates that quantitative analysis is also possible in this concentration range.

CONCLUSION

We succeeded in the separate detection of the components of 10 ppm of a BTX mixture gas by using our microfluidic device. We measured the changes in the absorption spectra of BTX mixture gas detected in a detection cell and found that the spectral shapes differ significantly with time due to the changes in the benzene, toluene, and *o*-xylene mixture ratio in the detected gas with time. We compared two types of silica adsorbent SDP and SBA-15, which have different pore structures. We found that the thermal desorption property differed with the adsorbent and SBA-15 provides better separation for each component than SDP. We concluded that the better separation with SBA-15 was due to an enhancement of the differences between the thermal desorption properties of benzene, toluene, and *o*-xylene caused by the repetition of the adsorption/desorption process in the nanosized column. As a result, we successfully realized the separate detection of the components of BTX mixture gases with our microfluidic device using a function of the nanosized pores of a porous adsorbent.

Received for review March 19, 2002. Accepted August 2, 2002.

AC0201732

(15) Kruk. M.; Jaroniec, M. *Chem. Mater.* **2000**, *12*, 1961. Yamada, T.; Zhou, H. S.; Asai, K.; Honma, I. *Mater. Lett.*, in press.